



FORMULATION AND INVITRO CHARACTERIZATION OF RH-VASCULAR ENDOTHELIAL GROWTH FACTOR LOADED SOLID LIPID NANOPARTICLES FOR HEALING CHRONIC WOUNDS

A. Sathyaraj^{1*}, Prof. M.V. Basaveswara Rao²

^{1*}Research Scholar, Department of Pharmacy, Krishna University, Machilipatnam, Andhra Pradesh, India.

²Professor, Department of Chemistry, Krishna University, Machilipatnam, Andhra Pradesh, India.

***Corresponding Author:** A. Sathyaraj

*Research Scholar, Department of Pharmacy, Krishna University, Machilipatnam, Andhra Pradesh, India.

Email: arsathya.pharma@gmail.com

Abstract:

Vascular endothelial growth factor (VEGF) is one of the most potent proangiogenic growth factors in the skin, and the amount of VEGF present in a wound can significantly impact healing. In this research study, rhVEGF (recombinant Vascular Endothelial Growth Factor) was epitomized into various lipid nanoparticles, i.e., SLN and NLC. In vitro tests were attempted in fibroblasts and keratinocytes to decide the bioactivity of the typified rh-VEGF and to gauge the cell take-up ability of the lipid nanoparticles, and their effectiveness was compared with that of a few intra-lesional organizations of a higher measurement of free rhVEGF and that of a solitary intra-lesional organization of rh-VEGF-loaded polylactic-co-glycolic corrosive (PLGA) and alginate microspheres (MS-rhVEGF) created in our research facility [26]. Mending was assessed as far as wound conclusion, recuperation of the incendiary stage, and re-epithelisation review.

Keywords: VEGF, Solid Lipid Nanoparticles, Invitro,

Introduction:

Since their first portrayal in the 1990s, lipid nanoparticles, basically solid-lipid nanoparticles (SLN) and nano-structured lipid carriers (NLC), have turned out to be intense medication conveyance frameworks that have pulled in much consideration and enthusiasm as effective and non-harmful transporters for different dynamic mixes [1,2]. Both lipid nanoparticles are reasonable for the assurance of medications against debasement, upgrade tranquilize soundness against light, oxidation, or hydrolysis, and give the supported arrival of dynamic mixes [3]. The fundamental contrast amongst SLN and NLC is the utilization of a fluid lipid (oil) for the planning of NLC which, as portrayed by a few creators, builds the stacking limit and diminishes spillage of the epitomized tranquilize amid capacity [1,2,4]. Lipid nanoparticles are generally utilized through various courses of organization for example, parenteral, oral, visual, and aspiratory organization) due to their superb averageness, biodegradability, and low harmfulness. These nanoparticles are

additionally reasonable conveyance frameworks for the topical treatment of skin maladies since they give high medication fixations in the treated skin zone. Moreover, foundational site effects may be lessened compared with the oral or parenteral organization courses because of the lower fundamental medication bioavailability gave by topical organization [5, 6]. In addition, their little molecule estimate and lipidic creation guarantee close contact between the nanoparticles and the skin, the discharge of the typified tranquilizes in a controlled way, and an expansion in their living arrangement time in the skin [7]. These particles additionally indicate occlusive properties that expansion skin hydration and upgrade sedate entrance [2,8,9]. Surprisingly, these particles permit the organization of hydrophilic sedates on the skin, which may enhance the topical treatment of skin infections [2, 10]. These qualities make the utilization of lipid nanoparticles as medication conveyance frameworks a fascinating and reasonable system for the treatment of chronic wounds. Truth be told, the occurrence of incessant wounds is ascending as an outcome of the maturing populace, making the change of ceaseless injury treatment a noteworthy medicinal services issue [11– 13]. Ceaseless injuries, for example, diabetic, venous, and weight ulcers, are those that are not ready to accomplish anatomic and useful trustworthiness of the harmed territory following a month and a half of standard medicinal treatment. Sadly, the topical organization of polymeric miniaturized scale and nanospheres was not found to demonstrate the normal accomplishment because of the quick spillage of the proteins from the injury site, bringing about the need to manage them once every day [24, 25]. To overcome these impediments and considering the reasonableness of lipid mixes for topical organization, the embodiment of GF into lipid nanoparticles may advance their organization as far as measurement, conveyance example, and wellbeing. Hence, these particles are introduced as a promising option for perpetual injury treatment.

Materials and methods:

Lipid nanoparticle preparation: SLN-rhVEGF and NLC-rhVEGF were prepared through the emulsification and ultrasonication-based method [27, 28]. For SLN-rhVEGF preparation, 10 ml of a 1% (w/v) Tween® 80 aqueous solution was mixed with 2 ml of a dichloromethane solution containing 0.1% (w/v) rhVEGF and 5% (w/v) Precirol® ATO 5. Immediately after mixing, the mixture was emulsified for 30 s at 50 W.

This step produced an o/w emulsion that was then stirred for 2 h to extract the organic solvent and allow particle formation. The SLN were then collected by centrifugation at 2,500 rpm for 10 min using a 100-kDa molecular weight cut-off centrifugal filter unit and washed three times with MilliQ water. After the addition of trehalose as a cryoprotectant at a concentration of 15% (w/w) of the weighed lipid, the SLNs were freeze-dried. For the preparation of NLC-rhVEGF, 100 µl of 20 mg/ml rhVEGF aqueous solution was added to a previously prepared blend composed of a warm aqueous solution of 0.67% (w/v) Poloxamer and 1.33% (w/v) Tween® 80 and a lipidic mixture containing 200 mg of melted Precirol® ATO 5 and 20mg of Miglyol®182 that was heated at 40 °C for 1 min. The resulting blend was emulsified for 15 s at 50W and stored for 12 h at 4 °C to recrystallise the lipid for NLC formation [29]. The particles were collected, washed, and lyophilized as previously described. The target loading of rhVEGF in both SLN-rhVEGF and NLC-rhVEGF was 1% (w/w). For the cell experiments, fluorescent lipid nanoparticles were prepared by incorporating 0.5% (w/w) Nile Red into the lipidic phase and following the method previously described.

Sterilization by Gamma(γ)-Irradiation of lipid nanoparticles:

SLN-rhVEGF and NLC-rhVEGF were sterilised by γ-irradiation (named SLN-rhVEGF γ and NLC-rhVEGF γ, respectively). The nanoparticles were placed in 5 ml glass vials and covered with dry ice to ensure a low temperature. A dose of 25 kGy from 60Co was used to ensure effective sterilisation in accordance with European Pharmacopeia recommendations [30]. The effect of the sterilisation process on the nanoparticle properties and the encapsulated rhVEGF was then studied.

Nanoparticle characterization:

SLN-rhVEGF and NLC-rhVEGF were disinfected by γ -light (named SLN-rhVEGF γ and NLC-rhVEGF γ , individually). The nanoparticles were put in 5 ml glass vials and secured with dry ice to guarantee a low temperature. A dosage of 25 kGy from ⁶⁰Co was utilized to guarantee viable sanitization as per European Pharmacopeia proposals [30]. The impact of the sanitization procedure on the nanoparticle properties and the embodied rhVEGF was then concentrated. The mean molecule estimate (z-normal) and polydispersity record (PDI) were estimated by powerful light dissipating. Each measure was performed in triplicate after nanoparticle lyophilisation. The zeta potential (ζ) was resolved through Laser Doppler smaller scale electrophoresis. The molecule morphology was resolved through checking electron microscopy and transmission electron microscopy (TEM) after negative recoloring. The nanoparticle portrayal additionally incorporated a physico-compound assessment of the pH, a thickness appraisal and an occlusivity test. The rheological investigations included the triplicate estimation of the thickness of 1 ml of the nanoparticle suspension at 0.5, 1, 2.5, and 5 rpm. Quickly, 5 ml of water was set in a Franz cell secured with a channel layer, and 10.6 mg/cm² nanoparticles were then connected to the channel surface to frame a film. Cells without test filled in as a kind of perspective. The samples were put away at 32 °C for 48 h and weighted toward the start and toward the finish of the analysis to get the water misfortune due to vanishing. The occlusion factor (F) was figured utilizing the accompanying condition using the following equation:

$$F (\%) = \frac{\text{Water loss without sample} - \text{Water loss with sample}}{\text{Water loss without sample}} \times 100.$$

Estimation of rhVEGF encapsulation Efficiency:

The encapsulation Efficiency (EE) was figured by implication by estimating the free rhVEGF (non-epitomized) evacuated through the filtration/centrifugation procedure depicted in Section 2.1. Each sample was then weakened 1:10,000 with DPBS arrangement containing 0.05% (v/v) Tween® 20 and 0.1% (w/v) BSA. The measure of free rhVEGF was evaluated utilizing a financially accessible Sandwich Enzyme-Linked Immunosorbent measure unit for human VEGF) following the producer's guidelines. The embodiment proficiency was surveyed utilizing the accompanying condition. All of the tests were performed in triplicate, and the results are reported as the means \pm S.D.

$$EE (\%) = \frac{\text{Initial amount of rhEGF} - \text{Free rhEGF}}{\text{Initial amount of rhEGF}} \times 100.$$

In vitro release studies:

The release study was conducted by incubating 32 mg and 23 mg of SLN-rhVEGF and NLC-rhVEGF, respectively (corresponding to \sim 200 μ g of rhVEGF), in 2 ml of 0.02 M phosphate-buffered saline (PBS) for three days. At selected intervals, the release medium was removed by filtration/ centrifugation and replaced by the same quantity of PBS [31]. The system was maintained under orbital rotation at 25 rpm, pH 7.4, and 37 \pm 0.5 °C. The amount of rhVEGF was assayed by ELISA using the protocol. The results are given in terms of the cumulative percentage of rhVEGF released over time.

In vitro cell culture studies:

Cell culture:

Balb/C 3T3 A31 fibroblasts were cultured on Dulbecco's modified Eagle's medium (DMEM) supplemented with 10% (v/v) foetal calf serum (FCS) and 1% (v/v) penicillin–streptomycin at 37 °C in a humidified incubator with a 5% CO₂ atmosphere. Human foreskin fibroblasts were cultured

on DMEM supplemented with 15% (v/v) foetal bovine serum (FBS), 1% (v/v) L-glutamine, and 1% (v/v) penicillin–streptomycin at 37 °C in a 5% CO₂ atmosphere. The cells were grown on DMEM supplemented with 10% (v/v) FBS, 1% (v/v) L-glutamine, and 1% antibiotic–antimycotic at 37 °C in a 5% CO₂ atmosphere.

Effect of rhVEGF-loaded nanoparticles on cell proliferation:

The effect of the rhVEGF-loaded nanoparticles on cell proliferation was assayed in Balb/C fibroblasts, which are widely used for the study of the bioactivity of rhVEGF [32, 33], and in human skin fibroblasts and human keratinocytes (HFF and HaCaT cell lines, respectively). The rhVEGF concentration of 15 ng/ml was chosen based on previously reported data [24, 34]. To perform the study, the Balb/C 3T3, HFF, or HaCaT cells were seeded in 24-well plates at a density of 50,000 cells/well in their respective complete culture medium. After 8 h of incubation, the medium was replaced by DMEM supplemented with 0.2% serum, and the plates were incubated overnight. The following samples were then added to the wells (all of the samples were resuspended in 0.2% serum-supplemented DMEM prior to their incorporation into the cell culture): (i) negative control (0.2% serum supplemented DMEM), (ii) 15 ng/ml of free rhVEGF, (iii) empty SLN, (iv) 15 ng/ml SLN-rhVEGF, (v) 15 ng/ml SLN-rhVEGF γ , (vi) empty NLC, (vii) 15 ng/ml NLC-rhVEGF, and (viii) 15 ng/ml NLC-rhVEGF γ . The cells were cultured under the same conditions for 24 h, 48 h, and 72 h. The experiments were performed in triplicate. After the different incubation intervals, 100 μ l of CCK-8 (Sigma-Aldrich, Saint Louis, USA) was added to the wells, and the mixture was incubated for 4 h [35]. The absorbance was then read at 450 nm and at 650 nm as the reference wavelength. The absorbance was directly proportional to the number of living cells in culture.

Cellular uptake of SLN-rhVEGF and NLC-rhVEGF

A total of 50,000 Balb/C 3T3, HFF and HaCaT were cultured separately on cover slips in their respective complete culture medium for 24 h. The medium was then replaced with the following assay mediums: (i) 25 μ g of SLN-Nile Red-rhVEGF in complete DMEM and (ii) 25 μ g of NLC-Nile Red-rhVEGF in complete DMEM. After 1 h of incubation, cells were washed twice with cold uptake buffer (0.14 M NaCl, 2 mM K₂HPO₄ and 0.4 mM KH₂PO₄) and once with cold acid buffer (0.26 M citric acid monohydrate, 80 mM sodium citrate and 85 mM KCl) and fixed with 3.7% paraformaldehyde. Nuclei were then stained with DAPI (500 ng/ml) and cover slips were mounted into the slides for examination in a fluorescence microscope (nuclear stain: DAPI excitation/emission 358/461 nm and particle stain: Nile Red excitation/ emission 530/605 nm).

Results and Discussion

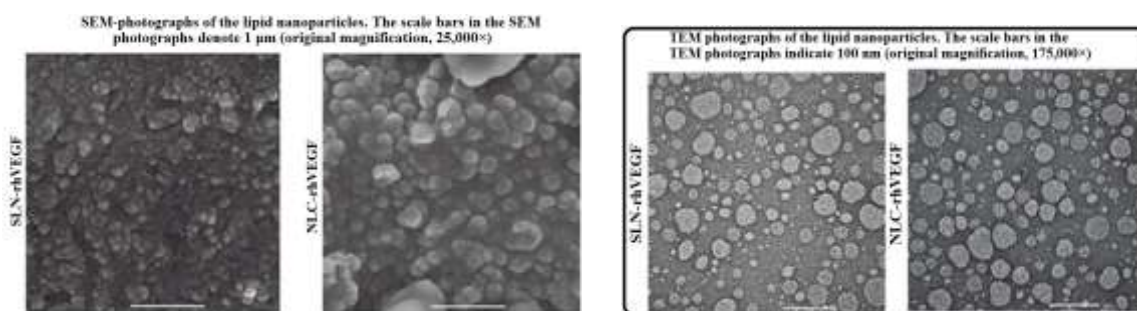
Nanoparticle characterization:

As depicted in Fig. 2A, the SLN and NLC with incorporated rhVEGF showed similar mean sizes: 332.45 ± 16.62 and 348.35 ± 10.25 , respectively. Remarkably, gamma sterilisation did not cause any significant change in the mean size or in the PDI of the lipid nanoparticles. The reconstitution of dry particles for the size measurements did not present any inconvenience, suggesting the absence of particle fusion or aggregation. The analysis of the zeta potential revealed that both formulations presented a similar surface charge of approximately 34 mV. In addition, as described by Pardeike et al., the data shown in Table 1 demonstrated that the NLC-rhVEGF preparation method resulted in improved drug entrapment because the EE values for NLC-rhVEGF and SLN-rhVEGF were $95.7 \pm 4.7\%$ and $73.9 \pm 2.2\%$, respectively ($p < 0.001$) [2]. These characteristics, together with the avoidance of the use of dichloromethane in the preparation of the NLC, may make NLC-rhVEGF a better alternative if its in vivo effectiveness is proved. Fig. 2B shows SEM and TEM photographs of the nanoparticles. In both formulations, the particles showed a smooth surface and similar size. The in vitro rhVEGF release profiles displayed in Fig. 2C show that both formulations presented similar release behaviors: an initial release (burst release) related to the percentage of surface-associated protein (SAP; $25.15 \pm 3.19\%$ for SLN-rhVEGF and $26.88 \pm 4.29\%$

for NLCrhVEGF), a fast release phase from 8 h to 24 h (~75% of the total rhVEGF), and a slower release phase from 24 to 72 h ending with the release of the total amount of rhVEGF. Moreover, it is worth mentioning that the in vitro release profile of the γ -sterilised nanoparticles did not differ from that of the non-sterilized ones. These data suggest the suitability of the final sterilization of SLN-rhVEGF and NLC-rhVEGF using gamma radiation. As depicted in Table 1, the nanoparticle characterization also revealed that the pH values of both formulations were within the range suitable for topical formulations (between 4 and 7), i.e., do not compromise the antimicrobial skin-barrier function observed with increased pH [42]. Moreover, the results from the occlusivity test described in Table 1 showed that the SLN were more occlusive than the NLC ($p < 0.05$). These results, as previously reported by Souto et al., may be attributed to the solid state of the lipid matrix of the SLN which may prevent more water evaporation than the semisolid matrix of the NLC. It should be noted that the occlusive properties of these formulations may allow their accumulation in the stratum corneum, resulting in the release of rhVEGF in a sustained manner and likely enhancing their therapeutic effect [4]. In addition, the rheological studies revealed that the SLN and NLC dispersions showed similar viscosity values of approximately $7 \times 10^3 \text{ Pa} \cdot \text{s}$ at 5 rpm and a pseudo-plastic behavior (decreasing viscosity with an increase in the shear rate).

Table:1: Results of the characterization of the developed formulations.

Parameter	SLN-rhEGF	NLC-rhEGF
Encapsulation efficiency (%)	73.9 ± 2.2	$95.7 \pm 4.7a$
pH	5.78 ± 0.12	5.85 ± 0.03
Occlusion factor (%)	18.08 ± 1.31	10.07 ± 0.63
Viscosity at 5 rpm ($\text{Pa} \cdot \text{s}$)	$6.67 \times 10^{-3} \pm 1.15 \times 10^{-4}$	$7.14 \times 10^{-3} \pm 9.02 \times 10^{-4}$
a: $p < 0.001$ compared with SLN-rhEGF. b: $p < 0.05$ compared with NLC-rhEGF. The data are shown as the means \pm S.D.		

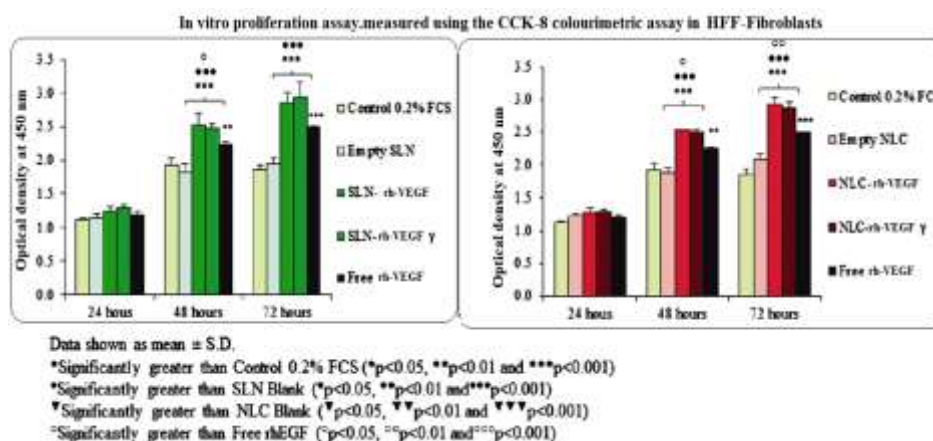
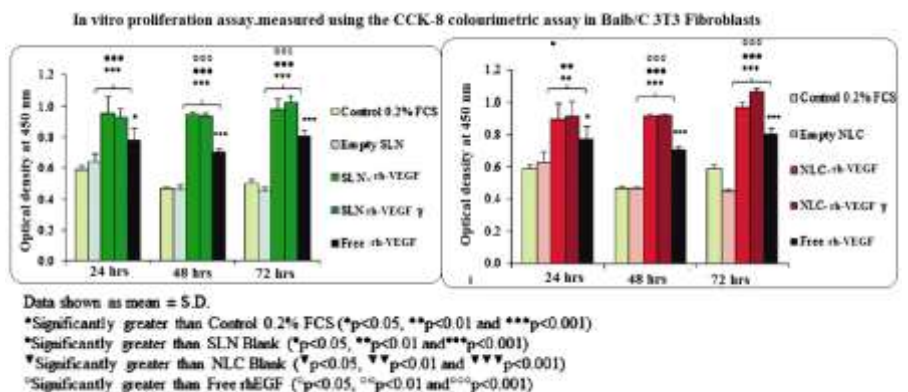


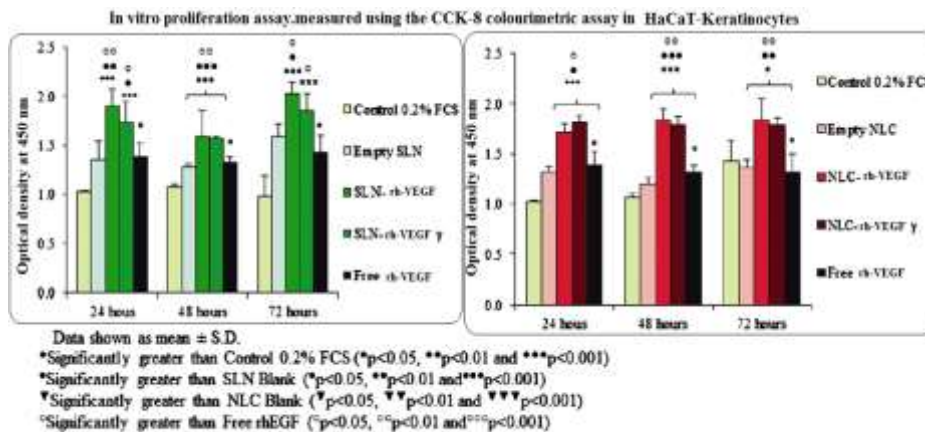
In vitro cell culture studies:

Effect of rhVEGF-loaded nanoparticles on cell proliferation:

The proliferation assays performed using Balb/c 3T3 fibroblasts, HFF fibroblasts, and HaCaT keratinocytes demonstrated the mitogenic effect of rhVEGF. The results, which are reported in Fig. 3A–C, indicated that the groups treated with rhVEGF (SLN-rhVEGF, SLN-rhVEGF γ , NLC-rhVEGF, NLCrhVEGF γ , and free rhVEGF) exhibited significantly higher cell proliferation than the control groups (0.2% FCS, empty SLN, and empty NLC) in all of the studied cell lines, illustrating that the nano-encapsulation process did not affect the biological activity of the growth factor ($p < 0.05$). These differences, as shown in Fig. 3A and C, were detectable starting from 24 h after treatment and became more evident at 48 and 72 h after treatment in the Balb/c fibroblasts and HaCaT keratinocytes. However, because the growth rate may depend on the cell line, the differences in HFF fibroblasts were not perceptible for the first 48 h (Fig. 3B). In addition, no differences were found between the lipid nano-particle-treated groups, regardless of sterilization. These data suggest that gamma sterilization is a potential alternative to aseptic processing, which

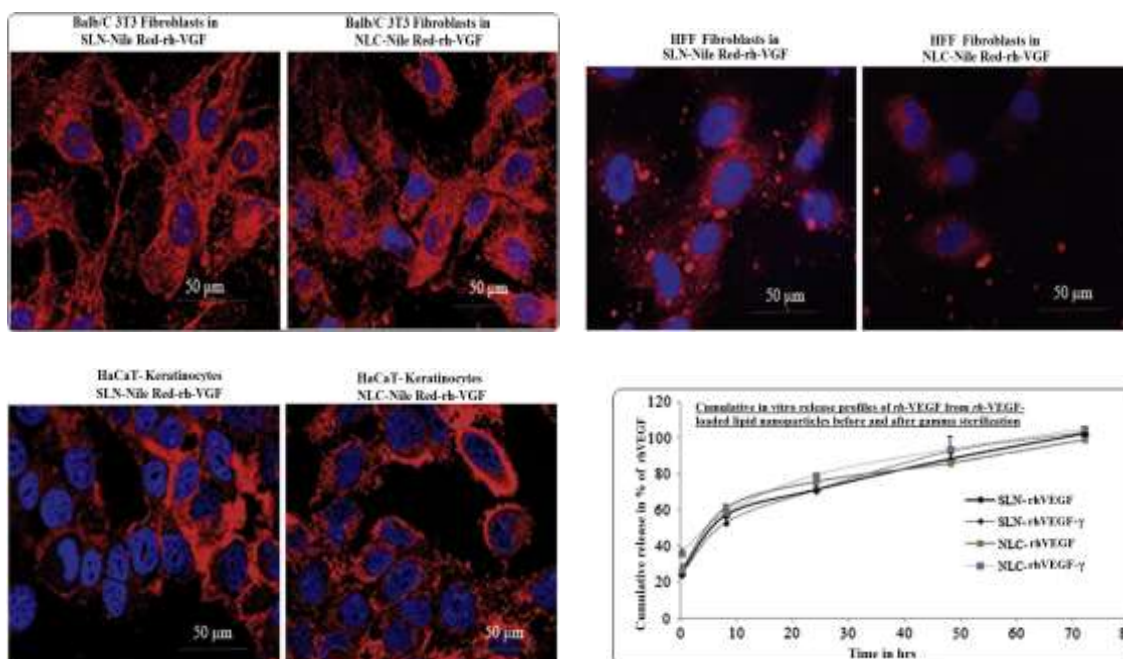
will facilitate future scale-up processes by reducing manufacturing costs. Nevertheless, the most striking result that emerged from these data is that the encapsulation of rhVEGF into nanoparticles (either SLN-rhVEGF or NLC-rhVEGF, regardless of irradiation) increased the mitogenic capability of all cell lines compared with that obtained with free rhVEGF: these differences were significant throughout the study for HaCaT keratinocytes and from 48 h to the end of the study for Balb/c and HFF fibroblasts ($p < 0.05$). These results suggest that nano-encapsulation may improve the growth factor stability and allow sustained delivery of rhVEGF, thereby permitting continuous binding to the cell surface VEGF receptor (VEGFR) and thus continuous activation of the signaling pathway of rhVEGF [24,43,44]. In contrast, the lower activity observed with free rhVEGF may be attributed to saturation of the VEGFR because the free rhVEGF may be administered at a much higher concentration than needed for the stimulation of the VEGFR [45]. Moreover, nano-encapsulation may promote nano-particle cell internalization and trafficking into the cytoplasm, nucleus, or some organelles [46]. All of these processes may impact the cell signaling pathway and thus cell proliferation [47]. Cellular uptake of SLN and NLC formulations because the nanoparticles are intended to be administered topically on damaged skin and will thus be in contact with skin keratinocytes and fibroblasts, the nano-particle cellular uptake was evaluated in the studied cell lines. The fluorescence microscope images shown in Fig. 4 revealed a high uptake of SLN-rhVEGF and NLC-rhVEGF in all of the cell lines. Both formulations were distributed throughout the cytoplasm and around the cellular membrane; in contrast, none of the formulations were detectable in the nucleus. From a qualitative perspective, no differences were found between the uptake capacity of SLN-rhVEGF and that of NLC-rhVEGF in the studied cell lines. As described in the literature, the rapid fading of Nile Red in hydrophilic environments is due to its lipophilic nature, which avoids the release of dye into cell culture medium [48]. Therefore, the fluorescence observed after the addition of the nanoparticles was a result of their cellular uptake and not due to the release of dye. In fact, the nano-particle cellular uptake of both





Cellular uptake of SLN and NLC formulations:

Because the nanoparticles are intended to be administered topically on damaged skin and will thus be in contact with skin keratinocytes and fibroblasts, the nanoparticle cellular uptake was evaluated in the studied cell lines. The fluorescence microscope images shown in Fig. 4 revealed a high uptake of SLN-rhVEGF and NLC-rhVEGF in all of the cell lines. Both formulations were distributed throughout the cytoplasm and around the cellular membrane; in contrast, none of the formulations were detectable in the nucleus. From a qualitative perspective, no differences were found between the uptake capacity of SLN-rhVEGF and that of NLC-rhVEGF in the studied cell lines. As described in the literature, the rapid fading of Nile Red in hydrophilic environments is due to its lipophilic nature, which avoids the release of dye into cell culture medium [48]. Therefore, the fluorescence observed after the addition of the nanoparticles was a result of their cellular uptake and not due to the release of dye. In fact, the nanoparticle cellular uptake of both SLN and NLC has been described by several researchers [49–51]. It is noteworthy to mention that the cellular uptake shown in Fig. 4 may be related to the increased cell proliferation observed in Section 3.2.1. In fact, as has been previously reported, the internalisation of the active compound into the cell cytoplasm is one of the possible strategies associated with bioactivity enhancement [46].



Conclusions

In the current work, SLN-rhVEGF and NLC-rhVEGF were developed, and their effectiveness was tested. The in vitro experiments revealed no loss of activity after the encapsulation or sterilization processes, which indicate that gamma sterilization is a suitable process for the final sterilisation of lipid nanoparticles. In the results demonstrate that the bioactivity of the nanoformulations was higher in all of the studied cell lines than that of 75 µg free rhVEGF. In addition, based on its EE and the lack of solvent utilization, 20 µg NLC-rhVEGF is a better alternative than SLNrhVEGF further animal studies are required to demonstrate the dose–response differences between 10 µg and 20 µg of nanoparticle-rhVEGF. Overall, these results suggest the promising future clinical application of rhVEGF-loaded lipid nanoparticles, especially NLC-rhVEGF, for the treatment of chronic wounds.

REFERENCES:

1. Emerich, D. F.; Thanos, C. G. The pinpoint promise of nanoparticle-based drug delivery and molecular diagnosis. *Biomol. Eng.*, **2006**, *23*, 171-184.
2. Ramanavicius, A.; Kausaite, A.; Ramanaviciene, A. Polypyrrole-coated glucose oxidase nanoparticles for biosensor design. *Sens. Actuat. B: Chem.*, **2005**, *111-112*, 532-539.
3. Jamieson, T.; Bakhshi, R.; Petrova, D.; Pockock, R.; Imani, M.; Seifalian, A. M. Biological applications of quantum dots. *Biomaterials*, **2007**, *28*, 4717-4732.
4. [Goldberg, M.; Langer, R.; Jia, X. Nanostructured materials for applications in drug delivery and tissue engineering. *J. Biomater. Sci. Polym. Ed.*, **2007**, *18*, 241-268.
5. Farokhzad, O. C.; Langer, R. Impact of nanotechnology on drug delivery. *ACS Nano*, **2009**, *3*, 16-20.
6. Blasi, P.; Giovagnoli, S.; Schoubben, A.; Ricci, M.; Rossi, C. Solid lipid nanoparticles for targeted brain drug delivery. *Adv. Drug Deliv. Rev.*, **2007**, *59*, 454-477.
7. Liu, W.; Hu, M.; Liu, W.; Xue, C.; Xu, H.; Yang, X. Investigation of the carbopol gel of solid lipid nanoparticles for the transdermal iontophoretic delivery of triamcinolone acetate. *Int. J. Pharm.*, **2008**, *364*, 135-141.
8. [8] Sung, J. C.; Pulliam, B. L.; Edwards, D. A. Nanoparticles for drug delivery to the lungs. *Trends Biotechnol.*, **2007**, *25*, 563-570.
9. Tan, A.; De La Peña, H.; Seifalian, A. M. The application of exosomes as a nanoscale cancer vaccine. *Int. J. Nanomed.*, **2010**, *5*, 889-900.
10. Kocbek, P.; Obermajer, N.; Cegnar, M.; Kos, J.; Kristl, J. Targeting cancer cells using PLGA nanoparticles surface modified with monoclonal antibody. *J. Control. Release*, **2007**, *120*, 18-26.
11. Ye, J.; Wang, Q.; Zhou, X.; Zhang, N. Injectable actarit-loaded solid lipid nanoparticles as passive targeting therapeutic agents for rheumatoid arthritis. *Int. J. Pharm.*, **2008**, *352*, 273-279.
12. Chung, Y. I.; Tae, G.; Hong Yuk, S. A facile method to prepare heparin functionalized nanoparticles for controlled release of growth factors. *Biomaterials*, **2006**, *27*, 2621-2626.
13. Musumeci, T.; Ventura, C. A.; Giannone, I.; Ruozi, B.; Montenegro, L.; Pignatello, R.; Puglisi, G. PLA/PLGA nanoparticles for sustained release of docetaxel. *Int. J. Pharm.*, **2006**, *325*, 172-179.
14. Haley, B.; Frenkel, E. Nanoparticles for drug delivery in cancer treatment. *Urol. Oncol.*, **2008**, *26*, 57-64.
15. Maeda, H.; Bharate, G. Y.; Daruwalla, J. Polymeric drugs for efficient tumor-targeted drug delivery based on EPR-effect. *Eur. J. Pharm. Biopharm.*, **2009**, *71*, 409-419.
16. Iyer, A. K.; Khaled, G.; Fang, J.; Maeda, H. Exploiting the enhanced permeability and retention effect for tumor targeting. *Drug Discov. Today*, **2006**, *11*, 812-818.
17. Brasnjevic, I.; Steinbusch, H. W. M.; Schmitz, C.; Martinez-Martinez, P. Delivery of peptide and protein drugs over the blood-brain barrier. *Prog. Neurobiol.*, **2009**, *87*, 212-251.

18. Silva, G. A. Nanotechnology approaches for drug and small molecule delivery across the blood brain barrier. *Surg. Neurol.*, **2007**, *67*, 113-116.
19. Allard, E.; Passirani, C.; Benoit, J. P. Convection-enhanced delivery of nanocarriers for the treatment of brain tumors. *Biomaterials*, **2009**, *30*, 2302-2318.
20. Pasha, S.; Gupta, K. Various drug delivery approaches to the central nervous system. *Expert Opin. Drug Deliv.*, **2010**, *7*, 113-135.
21. Kusuhara, H.; Sugiyama, Y. Efflux transport systems for drugs at the bloodbrain barrier and blood-cerebrospinal fluid barrier (Part 2). *Drug Discov. Today*, **2001**, *6*, 206-212.
22. Ulbrich, K.; Hekmatara, T.; Herbert, E.; Kreuter, J. R. Transferrin- and transferrin-receptor-antibody-modified nanoparticles enable drug delivery across the blood-brain barrier (BBB). *Eur. J. Pharm. Biopharm.*, **2009**, *71*, 251-256.
23. Liu, Z.; Jiao, Y.; Wang, Y.; Zhou, C.; Zhang, Z. Polysaccharides-based nanoparticles as drug delivery systems. *Adv. Drug Deliv. Rev.*, **2008**, *60*, 1650-1662.
24. Jain, A. K.; Khar, R. K.; Ahmed, F. J.; Diwan, P. V. Effective insulin delivery using starch nanoparticles as a potential trans-nasal mucoadhesive carrier. *Eur. J. Pharm. iopharm.*, **2008**, *69*, 426-435.
25. Kim, S.; Kim, J. H.; Jeon, O.; Kwon, I. C.; Park, K. Engineered polymers for advanced drug delivery. *Eur. J. Pharm. Biopharm.*, **2009**, *71*, 420-430.
26. Chen, C.; Yu, C. H.; Cheng, Y. C.; Yu, P. H. F.; Cheung, M. K. Biodegradable nanoparticles of amphiphilic triblock copolymers based on poly(3-hydroxybutyrate) and poly(ethylene glycol) as drug carriers. *Biomaterials*, **2006**, *27*, 4804-4814.
27. Liang, H. F.; Yang, T. F.; Huang, C. T.; Chen, M. C.; Sung, H. W. Preparation of nanoparticles composed of poly([gamma]-glutamic acid)- poly(lactide) block copolymers and evaluation of their uptake by HepG2 cells. *J. Control. Release*, **2005**, *105*, 213-225.
28. Byrne, J. D.; Betancourt, T.; Brannon-Peppas, L. ActiveJournal targeting schemes for nanoparticle systems in cancer therapeutics. *Adv. Drug Deliv. Rev.*, **2008**, *60*, 1615-1626.
29. Bajpai, A. K.; Shukla, S. K.; Bhanu, S.; Kankane, S. Responsive polymers in controlled drug delivery. *Prog. Polym. Sci.*, **2008**, *33*, 1088-1118.
30. [30] Ganta, S.; Devalapally, H.; Shahiwala, A.; Amiji, M. A review of stimuliresponsive nanocarriers for drug and gene delivery. *J. Control. Release*, **2008**, *126*, 187-204.
31. Rapoport, N. Physical stimuli-responsive polymeric micelles for anti-cancer drug delivery. *Prog. Polym. Sci.*, **2008**, *32*, 962-990.
32. [32] Pinto Reis, C.; Neufeld, R. J.; Ribeiro, A. J.; Veiga, F. Nanoencapsulation I. Methods for preparation of drug-loaded polymeric nanoparticles. *Nanomedicine*, **2006**, *2*, 8-21.
33. Bilati, U.; Allqmann, E.; Doelker, E. Development of a nanoprecipitation method intended for the entrapment of hydrophilic drugs into nanoparticles. *Eur. J. Pharm. Biopharm.*, **2005**, *24*, 67-75.
34. Budhian, A.; Siegel, S. J.; Winey, K. I. Haloperidol-loaded PLGA nanoparticles: Systematic study of particle size and drug content. *Int. J. Pharm.*, **2007**, *336*, 367-375.
35. Kim, D. H.; Martin, D. C. Sustained release of dexamethasone from hydrophilic matrices using PLGA nanoparticles for neural drug delivery. *Biomaterials*, **2006**, *27*, 3031-3037.
36. Jain, R. A. The manufacturing techniques of various drug loaded biodegradable poly(lactide-co-glycolide) (PLGA) devices. *Biomaterials*, **2000**, *21*, 2475-2490.
37. Feng, S. S.; Mei, L.; Anitha, P.; Gan, C. W.; Zhou, W. Poly(lactide)-vitamin E derivative/montmorillonite nanoparticle formulations for the oral delivery of Docetaxel. *Biomaterials*, **2009**, *30*, 3297-3306.
38. Chaloupka, K.; Malam, Y.; Seifalian, A. M. Nanosilver as a new generation of nanoprodut in biomedical applications. *Trends Biotechnol.*, **2010**, *28*, 580-8.
39. Pinto Reis, C.; Neufeld, R. J.; Ribeiro, A. n. J.; Veiga, F. Nanoencapsulation II. Biomedical applications and current status of peptide and protein nanoparticulate delivery systems. *Nanomedicine*, **2006**, *2*, 53-65.

40. Cohen-Sela, E.; Chorny, M.; Koroukhov, N.; Danenberg, H. D.; Golomb, G. A new double emulsion solvent diffusion technique for encapsulating hydrophilic molecules in PLGA nanoparticles. *J. Control. Release*, **2009**, *133*, 90-95.
41. Fonseca, C.; Simões, S.; Gaspar, R. Paclitaxel-loaded PLGA nanoparticles: preparation, physicochemical characterization and *in vitro* anti-tumoral activity. *J. Control. Release*, **2002**, *83*, 273-286.
42. Ceruti, M.; Crosasso, P.; Brusa, P.; Arpicco, S.; Dosio, F.; Cattel, L. Preparation, characterization, cytotoxicity and pharmacokinetics of liposomes containing water-soluble prodrugs of paclitaxel. *J. Control. Release*, **2000**, *63*, 141-153.
43. McCarron, P. A.; Marouf, W. M.; Quinn, D. J.; Fay, F.; Burden, R. E.; Olwill, S. A.; Scott, C. J. Antibody targeting of camptothecin-loaded PLGA nanoparticles to tumor cells. *Bioconjug. Chem.*, **2008**, *19*, 1561-1569.
44. [44] Panyam, J.; Zhou, W. Z.; Prabha, S.; Sahoo, S. K.; Labhasetwar, V. Rapid endo-lysosomal escape of poly(DL-lactide-co-glycolide) nanoparticles: implications for drug and gene delivery. *FASEB J.*, **2002**, *16*, 1217-1226.
45. Chang, J.; Jallouli, Y.; Kroubi, M.; Yuan, X. B.; Feng, W.; Kang, C. S.; Pu, P. Y.; Betbeder, D. Characterization of endocytosis of transferrin-coated PLGA nanoparticles by the blood-brain barrier. *Int. J. Pharm.*, **2009**, *379*, 285-292.
46. Gelperina, S.; Maksimenko, O.; Khalansky, A.; Vanchugova, L.; Shipulo, E.; Abbasova, K.; Berdiev, R.; Wohlfart, S.; Chepurnova, N.; Kreuter, J. Drug delivery to the brain using surfactant-coated poly(lactide-co-glycolide) nanoparticles: Influence of the formulation parameters. *Eur. J. Pharm. Biopharm.*, **2010**, *74*, 157-63.
47. Chavanpatil, M. D.; Patil, Y.; Panyam, J. Susceptibility of nanoparticle-encapsulated paclitaxel to P-glycoprotein-mediated drug efflux. *Int. J. Pharm.*, **2006**, *320*, 150-156.
48. [48] Xu, P.; Gullotti, E.; Tong, L.; Highley, C. B.; Errabelli, D. R.; Hasan, T.; Cheng, J. X.; Kohane, D. S.; Yeo, Y. Intracellular drug delivery by poly(lactic-co-glycolic acid) nanoparticles, revisited. *Mol. Pharm.*, **2008**, *6*, 190-201.
49. Fujita, H.; Banno, H.; Yamanouchi, D.; Kobayashi, M.; Yamamoto, K.; Komori, K. Pitavastatin Inhibits Intimal Hyperplasia in Rabbit Vein Graft. *J. Surg. Res.*, **2008**, *148*, 238-243.
50. Simosa, H. F.; Pomposelli, F. B.; Dahlberg, S.; Scali, S. T.; Hamdan, A. D.; Schermerhorn, M. L. Predictors of failure after angioplasty of infrainguinal vein bypass grafts. *J. Vasc. Surg.*, **2009**, *49*, 117-121.
51. Kimura, S.; Egashira, K.; Nakano, K.; Iwata, E.; Miyagawa, M.; Tsujimoto, H.; Hara, K.; Kawashima, Y.; Tominaga, R.; Sunagawa, K. Local delivery of imatinib mesylate (STI571)-incorporated nanoparticle *ex vivo* suppresses vein graft neointima formation. *Circulation*, **2008**, *118*, S65-S70.
52. Li, J.; Loh, X. J. Cyclodextrin-based supramolecular architectures: Syntheses, structures, and applications for drug and gene delivery. *Adv. Drug Deliv. Rev.*, **2008**, *60*, 1000-1017.
53. Du, Y. Z.; Xu, J. G.; Wang, L.; Yuan, H.; Hu, F. Q. Preparation and characteristics of hydroxypropyl- [beta]-cyclodextrin polymeric nanocapsules loading nimodipine. *Eur. Polymer J.*, **2009**, *45*, 1397-1402.
54. Agueros, M.; Areses, P.; Campanero, M. A.; Salman, H.; Quincoces, G.; Penuelas, I.; Irache, J. M. Bioadhesive properties and biodistribution of cyclodextrin-poly(anhydride) nanoparticles. *Eur. J. Pharm. Sci.*, **2009**, *37*, 231-240.
55. Memisoglu-Bilensoy, E.; Vural, I.; Bochet, A.; Renoir, J. M.; Duchene, D.; Hincal, A. A. Tamoxifen citrate loaded amphiphilic [beta]-cyclodextrin nanoparticles: *In vitro* characterization and cytotoxicity. *J. Control. Release*, **2005**, *104*, 489-496.